# A Modified-Square Slot Antenna with Circular Polarization Characteristics for Military Band Applications

Madhuri Sahal, Dinesh Yadav, Deepak Bhatnagar, and Manish Tiwari

*Abstract*— **In this work, the design and performance of a circularly polarized (CP) antenna designed using characteristic modal analysis (CMA) for military band application is presented. The substrate used is single-sided glass-reinforced epoxy and the antenna dimensions are 37×37×1.6 mm³. The antenna is compact, low-profile, circular polarized having an ARBW of around 500 MHz (center frequency 4.6 GHz). A coplanar waveguide (CPW) fed monopole antenna is used for excitation of the modified-square slot antenna that incorporates quarter section of circular symmetrical patches on the four corners. A stub orthogonal to the CPW fed monopole capacitively tunes the low Q mode as identified by CMA technique to shift to a lower frequency to create degenerate modes in military band for circular polarization generation. The 3-dB AR bandwidth of the antenna is in the frequency range 4.43-4.9 GHz and measured value of impedance bandwidth is 3.33 GHz. The fractional ARBW and impedance BW are 10.07 % and 61.6 % respectively. The peak antenna gain in the CP frequency band is 3.75 dBic. The proposed antenna exhibits good polarization purity, the minimum axial ratio is 1.38 at 4.6 GHz. The broad circular polarized antenna is suited for military applications covering the frequency range 4.43-4.9 GHz.**

*Index Terms*— **circular polarized, broadband, CMA, axial ratio, slot antenna.**

*Original Research Paper*
*DOI: 10.53314/ ELS2226046S*

## I. Introduction

Broadband circular polarized (CP) antennas have recently become popular for wireless communication applications owing to their robustness to adverse channel and weather conditions, faraday rotation, and polarization mismatch problems. The research community has shown great interest in planar circular polarized antennas for wireless applications due to easy fabrication, compact and low-profile configuration and hence easy integration in portable wireless devices.

Manuscript received 24 July 2021. Received in revised form 19 November 2021. Accepted for publication 23 December 2021

M. Sahal is with the Department of Electronics & comm Engineering, Manipal University Jaipur, Jaipur,(e-mail: madhuri.sahal@jaipur.manipal.edu)

D. Yadav is with the Department of Electronics & comm Engineering, Manipal University Jaipur, Jaipur (corresponding author to provide phone: +91-9829574400; e-mail: dinesh.yadav@jaipur.manipal.edu).

D. Bhatnagar is with the Department of Physics, University of Rajasthan, Jaipur, (e-mail: dbhatnagar2010@gmail.com).

M. Tiwari is with the Department of Electronics & comm Engineering, Manipal University Jaipur, Jaipur,(e-mail: manish.tiwari@jaipur.manipal.edu)

Near degenerate modes having equal amplitudes and orthogonal phase [1] must be excited for generating CP radiation. For attaining compact designs with circular polarization, several techniques have been implemented like current perturbations by using orthogonal peripheral slits [2], truncated corners [1], peripheral slits and truncated corners [3]-[5], loading asymmetrical length slots of different shapes [6]-[7] in orthogonal dimensions, fractal antenna structure [8], fractal defects in ground plane [9]. Though the design has a compact structure, the AR bandwidth obtained is less than 2.5 % [2], [4]-[9]. In [3], an axial ratio bandwidth of 5.8 % has been attained along with a size reduction of 6.6 %.

Generation of CP over a broad frequency range requires maintaining the orthogonality of phase over a wide frequency range in addition to their nearly equal amplitudes. The broadband circular polarized antenna design proposed in this work is uses CMA based insights to identify the degenerate modes required for circular polarization, which are then excited for wideband CP radiation. The antenna must be easily integrable in wireless devices and exhibit fairly good gain. Several recent works for the design of circular polarized antenna have used different techniques to generate the orthogonal degenerate modes that combine for CP generation. A square slot antenna has been designed on Rogers RO3003 substrate using an I-shaped radiator and modified ground plane having inverted L-shaped strip is proposed [10]. The design is very simple with a size of only $0.69\lambda_0 \times 0.69\lambda_0 \times 0.052\lambda_0$ and demonstrated an axial ratio bandwidth of around 36%. A truncated edge circular polarized antenna on an inclined ground plane [11] has been used for wideband CP generation at the cost of gain. Use of antenna ground plane to obtain the orthogonal phase relationship required for the two degenerate modes is carried in [12]-[13] the technique is suited to specific applications as it is limited by the ground dimensions. A compact antenna using the low cost FR4 substrate has been proposed by Haiyan Piao [14]. The antenna incorporates the use of PIFA for generating the linear polarized radiation characteristics. The orthogonal mode is excited by use of orthogonal branch to the PIFA. Phase quadrature between the modes is obtained through inductive effect of the shorting pin that connects the PIFA branch to ground plane and capacitive coupler at ground plane corner. Ground mode tuning structures have been used to tune resonances of degenerate modes by varying the inductance due to shorting pins to generate circular polarization characteristics. Though the antenna is compact with a ground size of $0.25\,\lambda_0 \times 0.25\,\lambda_0$, but it exhibits low gain 1.4 dB and narrow axial ratio bandwidth of 90 MHz (3.6 %). A simple design of monopole antenna utilizing parasitic loops and asymmetrical slot in ground plane [15] has been used to achieve CP characteristics. Though the design is very simple and demonstrates a good axial ratio bandwidth of 3.76GHz (83.9 %), the antenna bears large electrical size ($0.84\lambda_0 \times 0.84\lambda_0$) whereas gain is only 2.4 dBic.

The present communication demonstrates a new design of a glass-epoxy based, low-cost, planar wideband CP antenna based on CMA approach for military communication. The design is compact, has peak gain of 3.75 dBic and is useful for military band communication. The design is a modification of the basic wide slot antenna fed by a monopole as described in stage 1(initial stage) in [16]. The design is modified-square shaped slot antenna with circular corners and stubs protruding from edges of the square slot antenna for circular polarized radiation characteristics is presented. A stub orthogonally placed with respect to the monopole is used to enhance the impedance matching at desired frequency. This also generates the circular polarization characteristic and hence improves the AR bandwidth. The broadband circular polarized antenna presented in this work is useful for military applications like transfer of data/images captured during radio surveillance, communication, etc. The paper organization is as follows: section I includes brief introduction and motivation, section II(A) describes CMA based antenna design methodology, section II(B) refers to parametric study, section III relates to discussion of results & comparative analysis, section IV is conclusion.

## II. Antenna Design

The antenna design substrate used is easily available single-sided glass-reinforced epoxy ($\epsilon_r$ = 4.4 and tan δ = 0.025) having dimensions of 31 × 31 mm$^2$, and thickness 1.6 mm. Fig. 1 depicts the structure of proposed wideband CP antenna. The antenna design process involved simulations using FIT (Finite integration Technique) based transient solver of CST Microwave studio software with hexahedral meshing.

The steps involved in antenna designing are graphically represented in Fig. 2, whereas Fig. 3 depicts the changes in surface current at each subsequent stage at a frequency of 4.5 GHz. Fig. 4 depicts subsequent improvement in impedance matching performance and ARBW of the proposed antenna.

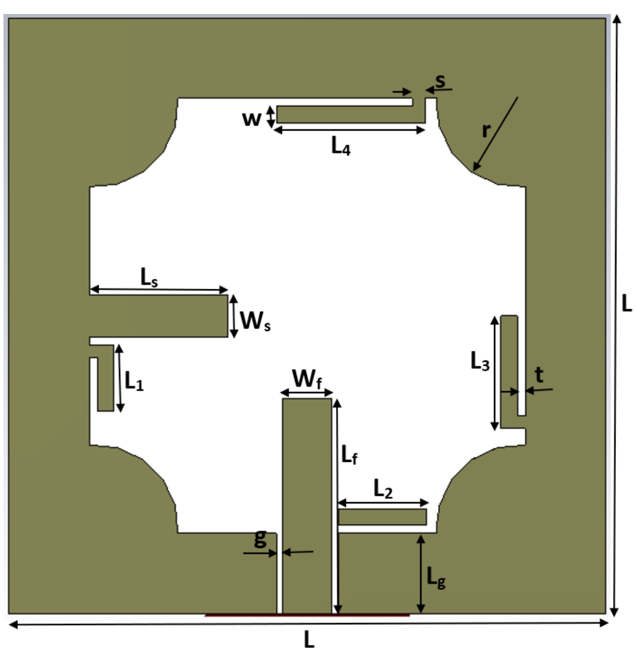


a)

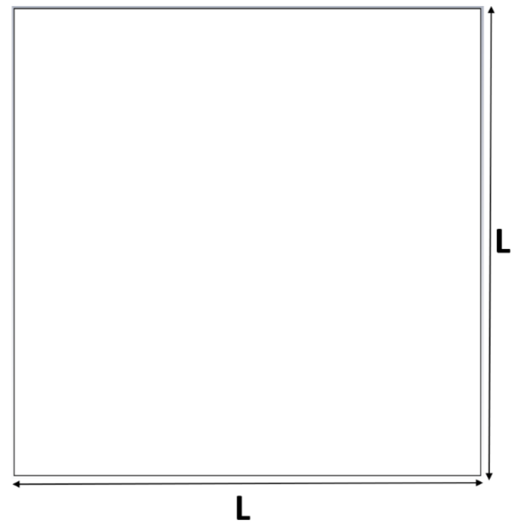


b)

Fig. 1. Proposed circular polarized military band antenna design (a) top view of geometry (b) bottom view of geometry.

### A. *Design Process*

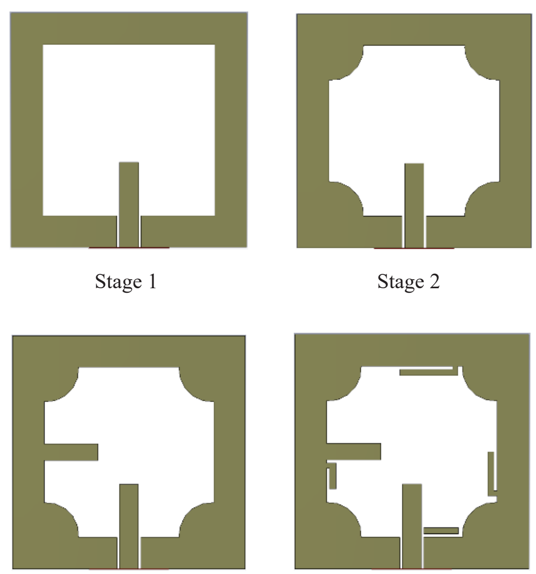


Fig. 2. Design process of the proposed circular polarized antenna

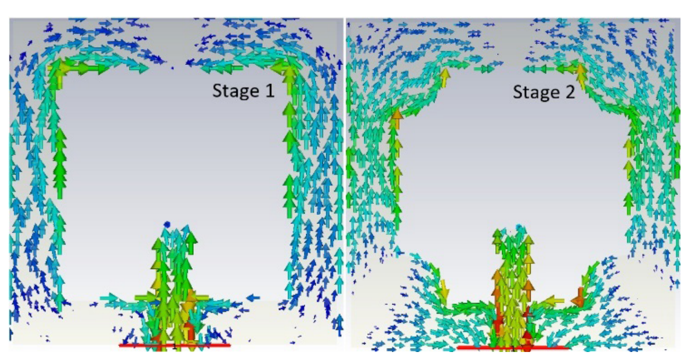

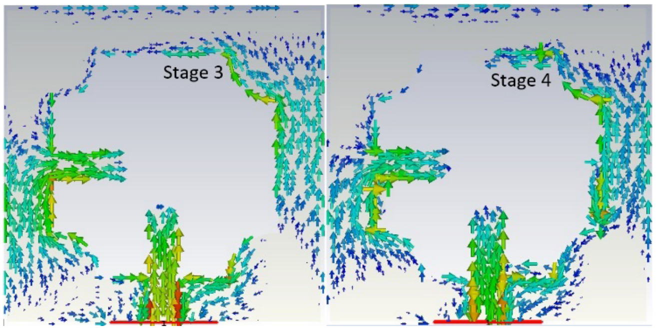


Fig. 3. Surface current at 4.5 GHz at each design stage of design process

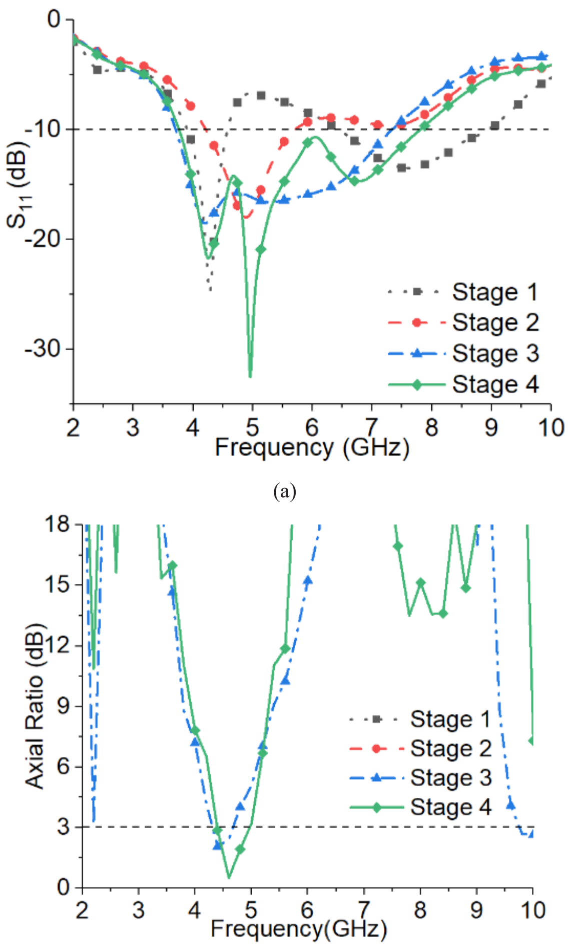


(a)

(b)

Fig. 4(a). Variation in Reflection coefficient with frequency (b). Variation in Axial ratio with frequency

Initial antenna design [16] is a square-shaped slot antenna designed for lowest frequency of operation in the desired circular polarized band. The square slot is excited using a CPW-fed monopole. The slot antenna bears a symmetrical current distribution in ground plane, thereby creating a strong vertical polarized radiation due to current in ground and monopole. The antenna in stage 1 exhibits resonance at around 4.2 and 7.5 GHz as in Fig 4(a). CMA analysis [17], [18] is performed for the antenna in stage 1 to obtain insights into the natural resonance frequencies of the antenna (Fig. 5). Modal significance [17] denoting the significant modes is represented by (1) below.

$$S_n = \left|\frac{1}{1+j\lambda_n}\right| \tag{1}$$

It can be inferred from Fig. 5 that the modes 3 and 4 are inherently low Q modes and therefore they must be excited and tuned to the desired frequency band so as to act as degenerate modes for CP generation.

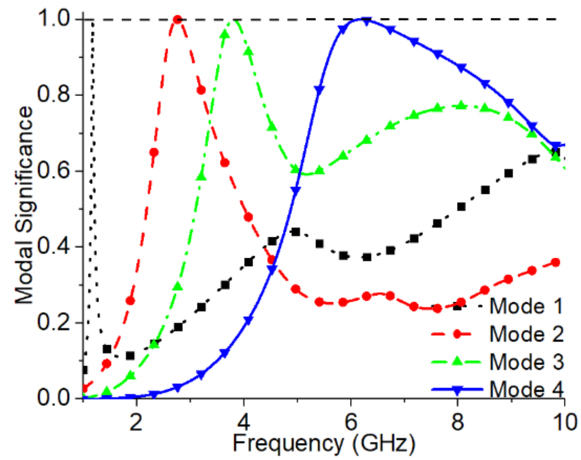


Fig. 5. Modal significance coefficient (Antenna in stage 1)

The basic antenna in stage 1 is a wide slot antenna modified by introducing symmetric circular quarter-sections having radii 5.1 mm in each of the corners as depicted in stage 2 to create a shorter path for current in antenna ground plane to increase the resonant frequency of mode 3 from around 4 GHz (as in Fig 5) to around 5 GHz (Fig 4 (a)). The symmetry in current distribution of ground plane remains intact and therefore antenna in stage 2 generates linear polarized radiation. The antenna design is further modified by introducing an orthogonal capacitive stub (stage 3) that lowers down the resonant frequency of mode 4 from around 6 GHz (as in Fig. 5) to nearly 5 GHz, thus exciting the modes 3 and 4 in the desired frequency range to cause CP operation. The current distribution in figure 4(b) depicts the strong horizontal component of current in the orthogonal stub that combines with the vertical current component generated by virtue of monopole in appropriate phase to generate CP. To improve the axial ratio bandwidth further, thin strips inductively coupled to antenna ground plane are introduced as depicted in stage 4. The antenna in stage 4 is circularly polarized over 4.39-4.97 GHz (fig. 4(b)). Subsequent to parametric optimization of the final stage 4 design for the given objectives, the final optimum dimensions are established as listed in Table 1.

B. *Parametric Optimization*

*Effect of stub length '$L_s$':* Effect of length of the orthogonal capacitive stub on impedance matching performance and axial ratio characteristics are studied (fig 6). The stub length is used to vary the amount of capacitance and thus the resonance frequency as in Fig. 6. It can also be used to tune to the desired center frequency for CP operation.

TABLE I
FINAL DIMENSIONS OF OPTIMIZED STRUCTURE

| Parameter | Value (mm) | Parameter | Value (mm) | Parameter | Value (mm) |
|---|---|---|---|---|---|
| L | 37 | $W_f$ | 3 | r | 5.1 |
| $L_g$ | 5 | $L_1$ | 4.1 | g | 0.3 |
| $L_s$ | 8.6 | $L_2$ | 5.5 | t | 0.5 |
| $W_s$ | 2.6 | $L_3$ | 7 | s | 0.8 |
| $L_f$ | 13.4 | $L_4$ | 8.4 | w | 1 |

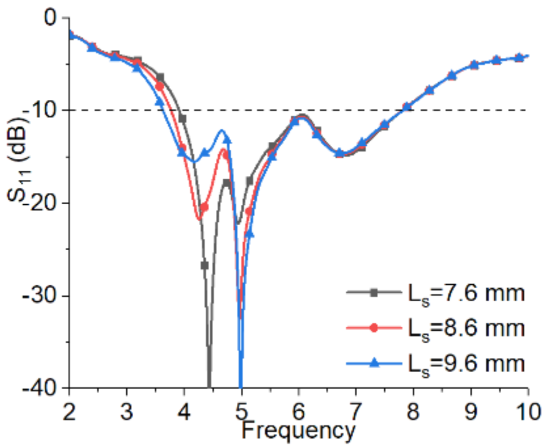


(a)

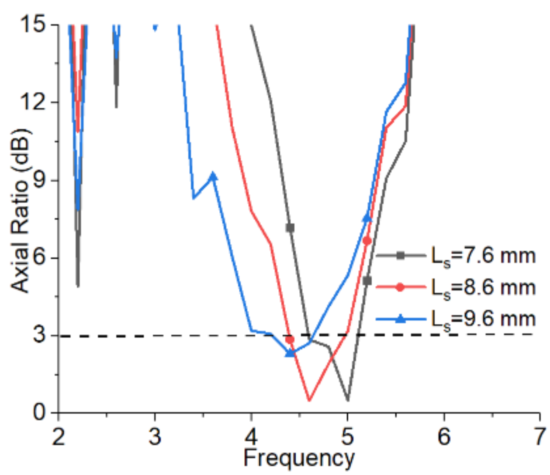


(b)

Fig. 6. Impact of stub length on (a) return loss (b) AR

*Effect of strip length '$L_3$' and '$L_4$'*: Strip lengths $L_3$ and $L_4$ can be used to fine tune the impedance matching and axial ratio characteristics as illustrated in Fig. 7 and Fig. 8 respectively. It can be inferred that $L_3$ and $L_4$ have significant impact on AR of the antenna as depicted in fig. 8.

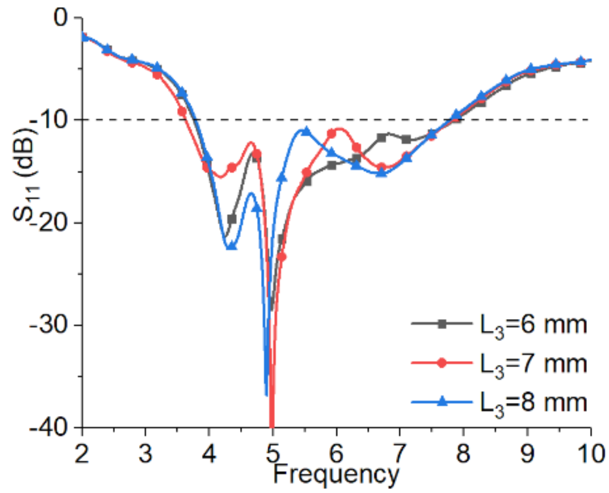


(a)

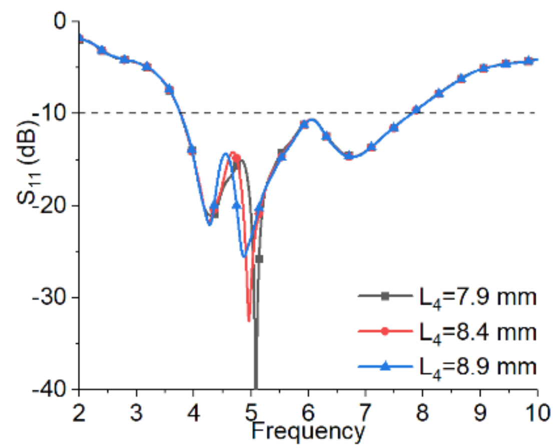


(b)

Fig 7. Impact of strip length (a) $L_3$ (b) $L_4$ on return loss

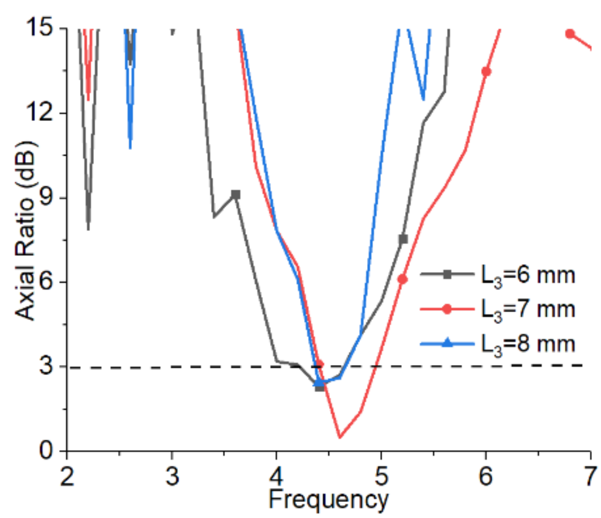


(a)

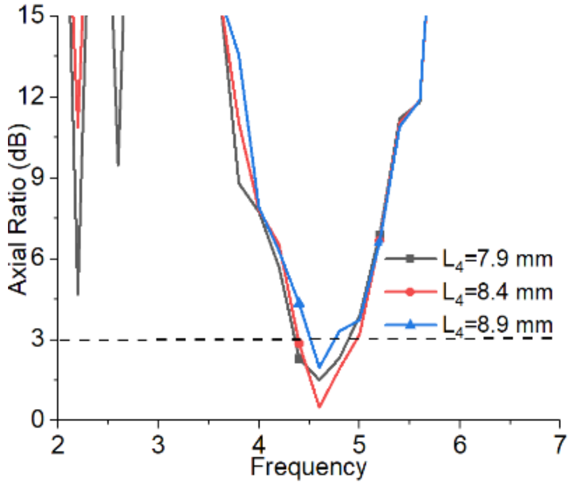


(b)

Fig. 8. Impact of strip length (a) $L_3$ (b) $L_4$ on axial ratio

## III. Results and Discussion

The wideband CP antenna prototype proposed in this work was fabricated on low cost FR4 substrate using conventional photolithography technique. The fabricated prototype is shown in Fig. 9 (a). The antenna reflection coefficients were measured using an Agilent Network Analyzer N5234A PNA-L connected to SMA port of antenna and the measured values were compared with the simulated reflection coefficient values in fig. 9. The antenna presented in this work is impedance matched for C-band and exhibits 10 dB impedance BW (measured) from 3.74 GHz to 7.07 GHz, as compared to a simulated impedance BW of 4 GHz from 3.79 GHz-7.79 GHz.

The far-field measurements of the antenna were performed in an anechoic chamber, the measured and simulated values of axial ratio and boresight gain are depicted in fig. 10. The measurements indicate a peak boresight gain of 3.75 dBic in the circular polarized band. The best value of measured axial ratio is 1.38 dB at 4.6 GHz, indicating good cross polar discrimination at the given frequency.

TABLE II
Performance Comparison With Recently Published CP Antennas. (*BW denotes bandwidth, $\lambda_0$ denotes wavelength at center frequency)

| Ref | Year | Centre frequency (GHz) | Absolute Impedance BW*, GHz (Fractional impedance*, %) | Axial ratio BW*, GHz (%) | Ground Size | Substrate used |
|---|---|---|---|---|---|---|
| [19] | 2015 | 3.89 | 0.54 (12.6%) | 0.13 (3.48%) | $\pi (0.38 \lambda_0)^2 \times 0.1 \lambda_0$ | Taconic (CER-10) |
| [20] | 2018 | 2.51 | 0.155 (6.2%) | 0.04 (1.6%) | $0.30\lambda_0 \times 0.30\lambda_0 \times 0.026 \lambda_0$ | RT duroid, $\varepsilon_r$=2.33 |
| [21] | 2015 | 0.91 | 0.037 (4.06 %) | 0.008 (0.87%) | $0.16\lambda_0 \times 0.16\lambda_0 \times 0.003\lambda_0$ | FR4 |
| [22] | 2012 | 2.45 | 0.8 (32.65%) | 0.1 (4.34%) | $0.45 \lambda_0 \times 0.40 \lambda_0$ | Rogers, $\varepsilon_r$=2.2 |
| [23] | 2011 | 5.9 | 10.33 (132%) | 2 (32.2%) | $1.19\lambda_0 \times 1.19\lambda_0 \times 0.015\lambda_0$ | FR4 |
| [24] | 2018 | 2.845 | 2.03 (71.35%) | 0.32 (14%) | $1.61 \lambda_0 \times 1.61 \lambda_0 \times 0.015 \lambda_0$ | $\varepsilon_r$=2.17 |
| [25] | 2014 | 1.61 | 0.09 (5.6%) | 0.035 (2.2%) | $0.32 \lambda_0 \times 0.32 \lambda_0 \times 0.027 \lambda_0$ | $\varepsilon_r$=3.4 |
| [26] | 2014 | 2.54 | 0.17 (6.7%) | 0.05 (1.96%) | $0.35 \lambda_0 \times 0.35 \lambda_0 \times 0.027 \lambda_0$ | Rogers, $\varepsilon_r$=2.2 |
| [27] | 2011 | 2.43 | ≈0.3 (12.5%) | ≈0.08 (3.2%) | $0.81 \lambda_0 \times 0.81 \lambda_0 \times 0.013 \lambda_0$ | FR4 |
| [28] | 2016 | 1.1 | 0.243 (22.4%) | 0.075 (6.8%) | $0.275\lambda_0 \times 0.275\lambda_0 \times 0.073\lambda_0$ | PTFE, $\varepsilon_r$=2.65 |
| [29] | 2018 | 3.02 | 0.18 (6%) | 0.13 (3.3%) | $1.525\lambda_0 \times 1.525\lambda_0 \times 0.016 \lambda_0$ | FR4 |
| [30] | 2017 | 5.7 | 2.8 (48.27%) | 0.7,0.45 (11.9 %, 6.8%) | $0.95 \lambda_0 \times 0.95 \lambda_0 \times 0.42 \lambda_0$ | RO4003, $\varepsilon_r$=3.55, |
| [31] | 2018 | 1.57 | 0.027 (1.71 %) | 0.01 (0.63 %) | $0.21 \lambda_0 \times 0.21 \lambda_0 \times 0.016 \lambda_0$ | F4BK350, εr = 3.5 |
| [32] | 2018 | 0.92 | 0.05 (5.43%) | 0.012 (1.3%) | $0.21 \lambda_0 \times 0.21 \lambda_0 \times 0.01 \lambda_0$ | FR4 |
| [33] | 2016 | 5.8 | 0.9 (15.5%) | 0.21 (3.6%) | $0.67 \lambda_0 \times 0.67 \lambda_0 \times 0.03 \lambda_0$ | $\varepsilon_r$=3.67 |
| **proposed** | **2021** | **4.7** | **3.33 (61.6 %)** | **0.47 (10.07%)** | $\mathbf{0.56 \lambda_0 \times 0.50 \lambda_0 \times 0.029 \lambda_0}$ | **FR4 substrate** |

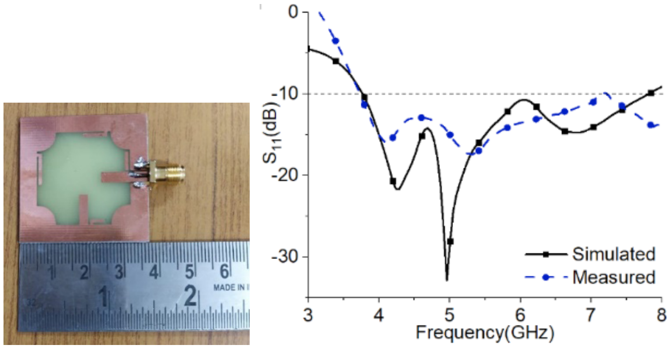

(a) (b)

Fig. 9 (a) Fabricated prototype (b) measured vs simulated return loss coefficients of proposed structure

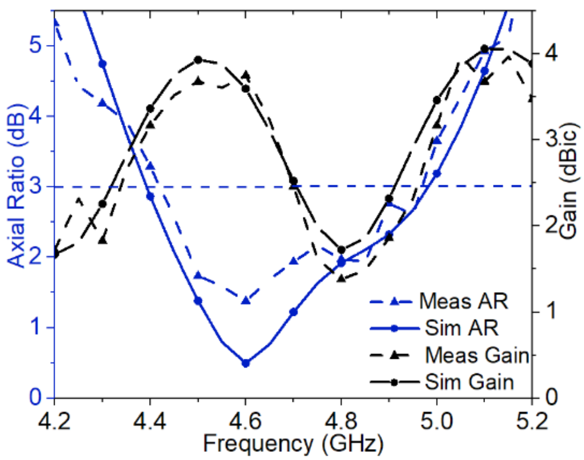


Fig. 10 Measured and simulated axial ratio and boresight gain

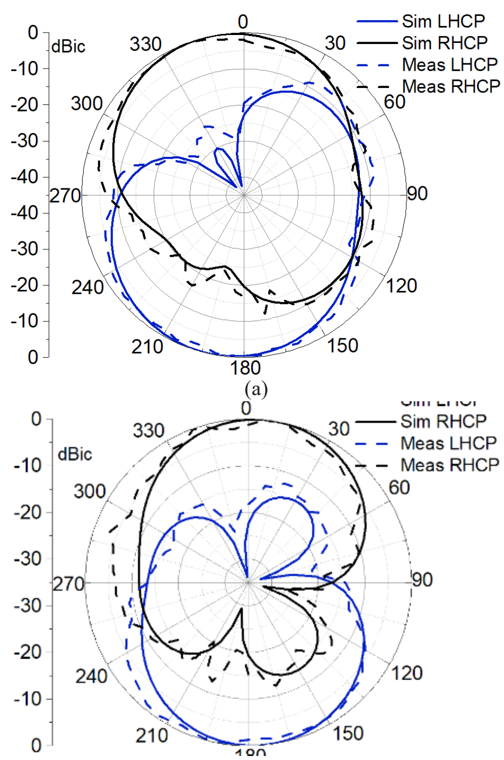

(a)

(b)

Fig. 11 (a) E-plane and (b) H-plane normalized measured and simulated radiation patterns at 4.5 GHz

The far-field 2-D radiation patterns at 4.5 GHz are depicted in fig. 11, the patterns indicates bidirectional radiation by the antenna. The radiation pattern indicates that the antenna is right-hand CP in +z-direction with a 3-dB AR beamwidth of 90º in E-plane and 55º in the H-plane. The proposed antenna emantes left-hand CP radiation in -z-direction.

A performance comparison of circular polarized antenna proposed in this work with few recently published works is presented in Table 2. below. The proposed antenna exhibits wide fractional impedance bandwidth and AR bandwidth with compact antenna dimension. The antenna exhibits a peak gain of 3.75 dBic in the CP band and is useful for military band communication.

## III. Conclusion

The paper includes the sequential design procedure using CMA technique and parametric analysis of the proposed design. The proposed antenna dimensions are 31 × 31 × 1.6 mm$^3$. The antenna is single-fed, compact and low-profile (0.029 $\lambda_0$), making it easy to integrate into portable wireless devices. The proposed antenna prototype has been tested; the results are found to be in close agreement. The antenna displays a wide AR beamwidth of 90° at 4.5 GHz and a peak gain of 3.75 dBic is attained. This makes it suitable for use in phased arrays for airborne communication in military band.

## Acknowledgment

The authors are extremely grateful to Late. Prof. V. N. Tiwari for his invaluable support and guidance for this research work. The authors acknowledge and are grateful to the Department of Electronics & Communication Engineering at Govt. Women's Engineering College, Ajmer for providing access to the antenna measurement facility at their institute.

## References


[1] K. L. Wong, *Compact and Broadband Microstrip Antennas*, John Wiley and Sons, 2002.

[2] K. Qian, X. Tang, "Compact LTCC dual-band circularly polarized perturbed hexagonal microstrip antenna", *IEEE Antennas Wirel. Propag. Lett.*, vol. 10, pp. 1212–1215, 2011.

[3] S. Mathew, R. Anitha, U. Deepak, C. K. Aanandan, P. Mohanan, K. Vasudevan, "A compact tri-band dual-polarized corner-truncated sectoral patch antenna", *IEEE Trans. Antennas Propag.,* vol. 63, pp. 5842–5845, 2015.

[4] W. S. Chen, C. K. Wu, K. L. Wong, "Novel compact circularly polarized square microstrip antenna", *IEEE Trans. Antennas Propag.*, vol. 49, pp. 340–342, 2001.

[5] D. L. Nguyen, K. S. Paulson, N. G. Riley, "Reduced-size circularly polarised square microstrip antenna for 2.45 GHz RFID applications", *IET Microwaves, Antennas Propag.*, vol. 6, pp. 94–99, 2012.

[6] Nasimuddin, X. Qing, Z. N. Chen, "A compact circularly polarized slotted patch antenna for GNSS applications", *IEEE Trans. Antennas Propag.*, vol. 62, pp. 6506–6509, 2014.

[7] Nasimuddin, X. Qing, Z. N. Chen, "A compact dualband circularly polarized GNSS antenna", *2017 Progress in Electromagnetics Research Symposium-Fall (PIERS-FALL)*, IEEE, 2017.

[8] N. R. Pasumarthy, P. R., Yagateela, "Compact single feed circularly polarized Koch island microstrip antenna", *AEU - Int. J. Electron. Commun.*, vol. 70, pp. 1543–1550, 2016.

[9] S. K. Pandey, G. P. Pandey, P. M. Sarun, "Circularly polarized micro-strip antenna with fractal trees loaded ground plane", *Electromagnetics*, vol. 39, pp. 505–523, 2019.

[10] Jaiverdhan, M. M. Sharma, and R. P. Yadav, "CPW Fed Ultra-Wideband Square Slot Antenna with Wideband Circular Polarization," in *2019 IEEE Asia-Pacific Microwave Conference(APMC)*, 2019, pp. 446–448.

[11] K. U. Sam, P. Abdulla, "Truncated circular microstrip ultra wideband antenna exhibiting wideband circular polarization", *Prog. Electromagn. Res. , C*, vol. 99, pp.111–122, 2020.

[12] Z. Liang, Y. Li, Y. Long, "Multiband monopole mobile phone antenna with circular polarization for GNSS application", *IEEE Trans. Antennas Propag.,* vol. 62, pp. 1910–1917, 2014.

[13] Z. Zahid, L. Qu, H. H. Kim, H. Kim, "Circularly polarised loop-type ground radiation antenna for mobile devices using a resonance inductor and capacitor", *Electronics Letters*, vol. 54, pp. 262-264, 2018.

[14] H. Piao, G. Dong, L. Qu, "Circularly polarized antenna using ground-mode tuning technique for small-sized IoT devices", *J. Electromagn. Waves Appl*., vol. 33, pp. 1042-1051, 2019.

[15] G. Feng, L. Chen, X. Shi, "A broadband circularly polarized monopole antenna employing parasitic loops and defective ground plane", *Microwave and Optical Technology Letters*, vol. 62, pp. 251-256, 2020.

[16] M. S. Ellis, Z. Zhao, J. Wu, X. Ding, Z. Nie, and Q.-H. Liu, "A Novel Simple and Compact Microstrip-Fed Circularly Polarized Wide Slot Antenna With Wide Axial Ratio Bandwidth for C-Band Applications," *IEEE Trans. Antennas Propag.*, vol. 64, no. 4, pp. 1552–1555, 2016.

[17] C.-F. Wang, Y. Chen, *Characteristic Modes-Theory and Applications in Antenna Engineering*, John Wiley and Sons, 2015.

[18] R. F. Harrington, J. R. Mautz, "Theory of Characteristic Modes for conducting Bodies", *IEEE Trans. Antennas Propag.*, vol. 19, pp. 622–628, 1971.

[19] K. B. Ng, C. H. Chan, K. M. Luk, "Low-cost vertical patch antenna with wide axial-ratio beamwidth for handheld satellite communications terminals", *IEEE Trans. Antennas Propag.,* vol. 63, pp. 1417–1424, 2015.

[20] Y. P. Rangaiah, R. V. S. Satyanarayana, P. N. Rao, "The effect of aspect ratio and fractal dimension of the boundary on the performance of fractal shaped CP microstrip antenna", *Prog. Electromagn. Res., M*, vol. 64, pp. 23–33, 2018.

[21] A. Farswan, A. K., Gautam, B. K., Kanaujia, K., Rambabu, "Design of Koch fractal circularly polarized antenna for handheld UHF RFID reader applications", *IEEE Trans. Antennas Propag*., vol. 64, pp. 771–775, 2015.

[22] A. Ghobadi, M. Dehmollaian, "A printed circularly polarized Y-shaped monopole antenna", *IEEE Antennas Wirel. Propag. Lett.*, vol. 11, pp. 22–25, 2011.

[23] J. Pourahmadazar, C. H. Ghobadi, J. Nourinia, N. Felegari, H. Shirzad, "Broadband CPW-fed circularly polarized square slot antenna with inverted-L Strips for UWB applications", *IEEE Antennas Wirel. Propag. Lett.,* vol. 10, pp. 369–372, 2011.

[24] F. Kurniawan, J. T. S. Sumantyo, S., Gao, K. Ito, C. E. Santosa, "Square-shaped feeding truncated circularly polarised slot antenna", *IET Microwaves, Antennas Propag.,* vol. 12, pp. 1279–1286, 2018.

[25] X. Qing, Z. N. Chen, "A compact circularly polarized slotted patch antenna for GNSS applications", *IEEE Trans. Antennas Propag.*, vol. 62, pp. 6506–6509, 2014.

[26] V. V. Reddy, N. V. S. N. Sarma, "Compact circularly polarized asymmetrical fractal boundary microstrip antenna for wireless applications", *IEEE Antennas Wirel. Propag. Lett.,* vol. 13, pp. 118–121, 2014.

[27] J. Row, T., Lee, M.,Chen, "Circularly-polarized ring slot antenna fed by a V-shaped coupling strip", *IEEE Trans. Antennas Propag.*, pp. 1-5, 2011.

[28] X. Chen, L. Yang, J. Y. Zhao, G. Fu, "High-efficiency compact circularly polarized microstrip antenna with wide beamwidth for airborne communication", *IEEE Antennas Wirel. Propag. Lett*., vol. 15 , pp. 1518–1521, 2016.

[29] J. F. Lin, Q. X. Chu, "Enhancing bandwidth of CP microstrip antenna by using parasitic patches in annular sector shapes to control electric field components", *IEEE Antennas Wirel. Propag. Lett*., vol. 17, pp. 924–927, 2018.

[30] T. D. Bui, Q. C. Nguyen, M. T. Le, "Novel wideband circularly polarized antenna for wireless ap plications", *Proceedings of 2017 Asia Pacific Microwave Conference*, IEEE, pp. 430–433, 2017.

[31] M. S. Wang, X. Q. Zhu, Y. X. Guo, W. Wu, "Compact circularly polarized patch antenna with wide axial ratio beamwidth", *IEEE Antennas Wirel. Propag. Lett*., vol. 17, pp. 714-718, 2018.

[32] X. Yang, Q. Feng, Z. Zheng, "First-order minkowski fractal circularly polarized slot loop antenna with simple feeding network for UHF RFID reader", *Prog. Electromagn. Res.*, vol. 77, pp. 89–96, 2018.

[33] S. Maddio, "A compact circularly polarized antenna for 5.8-GHz intelligent transportation system", *IEEE Antennas Wirel. Propag. Lett.*, vol. 16, pp. 533-536, 2016.